Pergamon

Int. J. Heat Mass Transfer. Vol. 40, No. 15, pp. 3641–3652, 1997

Printed in Great Britain
0017–9310/97 $17.00+0.00

PII: S0017–9310(97)00006–9

Effect of wall conduction on natural convection flow of micropolar fluids along a flat plate

MING-I CHAR and CHENG-LONG CHANG

Department of Applied Mathematics, National Chung Hsing University, Taichung, Taiwan 402, Republic of China

(*Received* 10 *May* 1996 *and in final form* 26 *November* 1996)

Abstract—This article numerically studies the coupling of wall conduction with laminar free convective heat transfer of micropolar fluids along a vertical flat plate. The governing boundary layer equations along with the boundary conditions are first cast into a dimensionless form by a nonsimilar transformation and the resulting equations are then solved by the cubic spline collocation method. The effects of the conjugate heat transfer parameter p, the micropolar material parameter Δ and the Prandtl number Pr on the flow and thermal fields are discussed in detail. The results clearly indicate that the conjugate heat transfer parameter has a significant influence on the fluid flow and heat transfer characteristics in comparison with those reported for isothermal flat plate. The interfacial temperature increases monotonically along the streamwise direction. The conjugate heat transfer parameter is to reduce the solid–liquid interfacial temperature, the skin friction factor, the wall couple stress and the local heat transfer rate. The effect of wall conduction on the local heat transfer rate is more pronounced for a system with larger Prandtl numbers or smaller micropolar material parameters. In addition, comparing it to Newtonian fluids, a reduction in the skin friction factor and the local heat transfer rate is reported. © 1997 Elsevier Science Ltd.

INTRODUCTION

Study of free convection heat transfer in Newtonian fluids along a vertical plate is well-known. Its extensions to non-Newtonian fluids are important for the thermal design of industrial equipment dealing with molten plastics, polymeric liquids, foodstuffs, or slurries. Hence, considerable efforts have been directed toward this coupled, nonlinear boundary layer problem.

Eringen [1] proposed the theory of micropolar fluids, a sub class of micro-fluids, in which the microscopic effects arising from the local structure and micromotions of the fluid elements are taken into account. This theory can be used to analyze the behavior of exotic lubricants, polymeric fluids, liquid crystals, animal bloods, colloidal and suspension solutions, etc., for which the classical Navier–Stokes theory is inadequate. Flow motion of such fluids is described by a local microrotation vector together with the velocity vector. Eringen [2] later generalized the micropolar fluids theory to include thermal effects. A comprehensive review of the subject and application of micropolar fluid mechanics was given by Ariman *et al.* [3]. Ahmadi [4] obtained a similarity solution for the micropolar boundary layer flow over a semi-infinite plate. Jena and Mathur [5] further studied the laminar free convection in the boundary layer flow of the thermomicropolar fluids past a nonisothermal vertical flat plate.

In addition, Soundalgekar and Takhar [6] obtained a similarity solution for the flow and heat transfer past a continuously moving semi-infinite plate in a micropolar fluids. Gorla and Ameri [7] used the theory of micropolar fluids formulated by Eringen to investigate the mixed convection boundary layer flow on a continuous moving cylinder. The thermal boundary conditions of isothermal wall as well as constant wall heat flux are considered. Later, an analysis for steady mixed convection in micropolar boundary layer flow on a vertical flat plate with constant wall temperature or heat flux has been done by Gorla [8]. Gorla *et al.* [9] used the asymptotic expansion technique to study the mixed convection heat transfer of a micropolar fluid from a vertical isothermal plate. Consideration is given to the two regions, near to as well as far away from the leading edge. The effect of suction or injection on the heat transfer characteristics of a micropolar fluids flow past a stretching sheet with prescribed wall temperature has been studied by Hassanien and Gorla [10].

In the previous studies [5–10], the thermal boundary condition at the solid surface was assumed either prescribed wall temperature or prescribed heat flux and, thus, the interaction between the solid surface and its adjacent boundary-layer was neglected. Consideration of the coupled heat transfer processes between solid body (conduction mechanism) and the fluid flow (convection mechanism) is known as a conjugate heat transfer problem. Steady conjugate heat transfer of a Newtonian fluid along a solid surface has been investigated by several investigators. For example, Kelleher and Yang [11] provided an analytic solution of the natural convection boundary layer flow

NOMENCLATURE

b	thickness of the plate
B	dimensionless parameter of micro-inertia density
C_f	skin friction coefficient
C_p	specific heat
F	reduced stream function
g	gravitational acceleration
G	dimensionless microrotation
Gr	Grashof number
Gr_x	local Grashof number
$\bar{h}$	average heat transfer coefficient
j	micro-inertia density
K	thermal conductivity
L	length of the plate
M_w	dimensionless wall couple stress
N	angular velocity of micropolar fluid
$\overline{Nu}$	average Nusselt number
Nu_x	local Nusselt number
p	conjugate heat transfer parameter
Pr	Prandtl number
T	temperature
U_c	characteritic velocity
u, v	velocity components in x and y directions, respectively
x, y	rectangular coordinates.

Greek symbols

α	thermal diffusivity
β	thermal expansion coefficient
γ	spin-gradient viscosity
Δ	dimensionless parameter of vortex viscosity
η	pseudo-similarity variable
θ	dimensionless temperature
κ	vortex viscosity
λ	dimensionless parameter of spin-gradient viscosity
μ	dynamic viscosity
ν	kinematic viscosity
ξ	dimensionless streamwise coordinate
ρ	density of micropolar fluid
τ	shear stress.

Superscripts

n	false time level of n
$n+1$	false time level of $n+1$
$'$	derivate with respect to η.

Subscripts

f	condition in the fluid
s	condition in the plate
w	condition at solid–liquid interface
∞	condition in surrounding medium.

generated adjacent to a semi-infinite vertical slab with a finite thickness and an arbitrary distribution of heat sources. A theoretical analysis of the laminar natural convection from a tapered, downward-projecting fin was presented by Lock and Gunn [12]. A quasi-one-dimensional conduction was assumed in the fin and the boundary layer approximations were treated for the flow. Later, Zinnes [13] used a finite-difference procedure to study the problem of steady, two-dimensional, laminar natural convection from a vertical, heat-conducting flat plate of finite thickness with an arbitrary heating distribution on its surface. Chida and Katto [14] applied the method of vectorial dimensional analysis to find the dimensionless parameters which control the characteristics of the conjugate heat transfer.

Furthermore, Miyamoto *et al.* [15] studied, numerically and experimentally, two-dimensional conjugate heat transfer problems of free convection from a vertical flat plate with a uniform temperature or a uniform heat flux at the outside surface of the plate. Timma and Padet [16] used the extension of Blasius method to investigate the similar problem. In Ref. [16], a one-dimensional model for the plate conduction equation was considered in their analysis. Pozzi and Lupo [17] obtained the perturbation solutions for the coupled problem of natural convection along and conduction inside a heated flat plate. Recently, the effects of wall conduction on the characteristics of free convection between asymmetrically heated vertical plates were performed by Kim *et al.* [18, 19] for uniform wall heat flux and for uniform wall temperature, respectively. Their results showed that wall conduction effects are more pronounced for low Grashof number flows than for high Grashof number flows. Char *et al.* [20] analyzed, using the cubic spline collocation numerical method, the conjugate heat transfer occurring in the laminar boundary layer on a continuous, moving plate. More recently, Vynnycky and Kimura [21] made a systematic study on the two-dimensional conjugate free convection due to a vertical plate of finite extend adjacent to a semi-infinite fluid region. The problem of conjugate natural convection flow over the outside surface of a slender hollow circular cylinder was studied by Na [22]. The aforementioned investigations dealing with conjugate heat transfer problems [11–22] are for Newtonian fluids flow along a solid surface. The problem of conjugate natural convection flow of a micropolar fluid has not received attention. This has motivated the present study.

The purpose of this paper is to analyze the effect of

wall conduction on laminar natural convection heat transfer of micropolar fluids along a vertical flat plate. We shall follow the previous analyses [16–17, 22] by assuming a thin heated plate so that heat conduction within the plate is one-dimensional. A cubic spline method has been used to solve this conjugate heat transfer problem. Variations in the fluid–solid interfacial temperature distribution, the skin friction factor, the wall couple stress and the local heat transfer rate are presented to highlight the influence of the wall conduction. Comparisons with available published results for conjugate natural convection flow of Newtonian fluids along a vertical flat plate are also presented, in view of the interfacial temperature distributions.

MATHEMATICAL FORMULATION

Consider a vertical flat plate of length L and finite thickness b, which is placed in an extensive body of quiescent micropolar fluid. The physical model and coordinate system are shown in Fig. 1, where the streamwise coordinate is denoted by x and that normal to it is denoted by y. The temperature of the micropolar fluid far away from the plate is T_∞, whereas that of the outside surface of the plate is maintained at a constant temperature T_b and $T_b > T_\infty$.

In the formulation of the present problem the following common assumptions are made: the flow is steady, laminar, incompressible and two-dimensional; the effects of viscous dissipation and the micropolar heat conduction are neglected; and the boundary layer and Boussinesq approximations are valid. Under these assumptions, the governing equations for the flow field are [5, 9]:

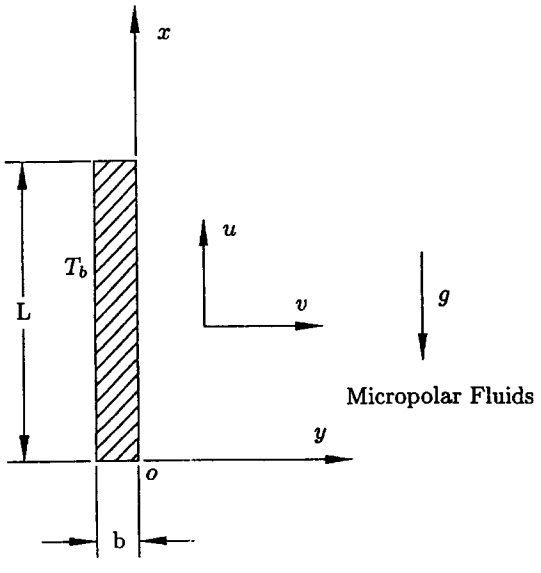

Fig. 1. The physical model and coordinate system.

continuity

$$\frac{\partial u}{\partial x}+\frac{\partial v}{\partial y}=0 \tag{1}$$

momentum

$$u\frac{\partial u}{\partial x}+v\frac{\partial u}{\partial y}=\left(\nu+\frac{\kappa}{\rho}\right)\frac{\partial^2 u}{\partial y^2}+\frac{\kappa}{\rho}\frac{\partial N}{\partial y}+\beta g(T-T_\infty) \tag{2}$$

angular momentum

$$u\frac{\partial N}{\partial x}+v\frac{\partial N}{\partial y}=-\frac{\kappa}{\rho j}\left(2N+\frac{\partial u}{\partial y}\right)+\frac{\gamma}{\rho j}\frac{\partial^2 N}{\partial y^2} \tag{3}$$

energy

$$\rho C_p\left(u\frac{\partial T}{\partial x}+v\frac{\partial T}{\partial y}\right)=K_f\frac{\partial^2 T}{\partial y^2}. \tag{4}$$

In the foregoing equations u and v are the velocity components along the x- and y-directions; ρ, ν, C_p and β are the density, kinematic viscosity, specific heat and the thermal expansion coefficient of the fluid; and κ, j and γ are the vortex viscosity, micro-inertia density and spin-gradient viscosity. Furthermore, T is the temperature, N is the component of microrotation whose direction of rotation is in the xy-plane, g is the acceleration due to the gravity and K_f is the thermal conductivity of the fluid.

The boundary conditions for equations (1)–(4) are:

$$u=v=0;\quad N=-\frac{1}{2}\frac{\partial u}{\partial y};\quad T=T_w(x) \qquad \text{at } y=0 \tag{5a}$$

$$u\to 0;\quad N\to 0;\quad T\to T_\infty \quad \text{as } y\to\infty \tag{5b}$$

where the subscripts w and ∞ refer to the wall and boundary layer edge, respectively, and the boundary condition (5a) for N at the plate, $y=0$, means that the microrotation equals half of the fluid vorticity at the boundary [4, 7]. $T_w(x)$ is the surface temperature of the plate, which is not known *a priori*.

It is noted that T_w depends on x; one objective of this work is to predicted $T_w(x)$ and one further governing equation is, therefore, required. The additional equation for the flat plate is based on the simplification that the plate is steadily transferring its heat to the surrounding micropolar fluid and the thickness of the plate b is small compared to its length L.

Under the above simplification, the axial conduction term in the heat conduction equation of the flat plate can be omitted [16, 17, 22]. Accordingly, the governing equation for temperature distribution within the plate is

$$\frac{\partial^2 T_s}{\partial y^2}=0;\quad 0\leqslant x\leqslant L;\quad -b<y\leqslant 0 \tag{6}$$

where T_s is the temperature in the plate. The boundary conditions for the plate are

$$T_s = T_b \quad \text{at } y = -b \tag{7a}$$

$$T_s = T(x,0); \quad -K_s\frac{\partial T_s}{\partial y} = -K_f\frac{\partial T(x,0)}{\partial y} \quad \text{at } y = 0. \tag{7b}$$

The boundary conditions (7b) state the physical requirements that the temperature and heat fluxes of the plate and the micropolar fluid must be continuous across the solid–fluid interface. By using equations (6) and (7), the temperature in the plate is given by

$$T_s = T(x,0) - (T_b - T(x,0))y/b. \tag{8}$$

It should be noted that $T(x,0)$ is the unknown temperature at the interface. Thus, the heat flux continuity condition at the interface may be written as

$$T_w(x) = T(x,0) = b\frac{K_f}{K_s}\frac{\partial T(x,0)}{\partial y} + T_b. \tag{9}$$

To facilitate the analysis, we now introduce pseudo-similarity variables (ξ,η) with the reduced stream function $F(\xi,\eta)$, the dimensionless microrotation $G(\xi,\eta)$, and the dimensionless temperature $\theta(\xi,\eta)$ as follows:

$$\xi = \frac{x}{L} \tag{10}$$

$$\eta = \frac{Gr^{1/4}}{L\xi^{1/4}}y \tag{11}$$

$$F(\xi,\eta) = \frac{\psi}{\nu Gr^{1/4}\xi^{3/4}} \tag{12}$$

$$G(\xi,\eta) = \frac{L^2}{\nu Gr^{3/4}\xi^{1/4}}N \tag{13}$$

$$\theta(\xi,\eta) = \frac{T-T_\infty}{T_b-T_\infty} \tag{14}$$

where Gr is the Grashof number

$$Gr = g\beta(T_b - T_\infty)L^3/\nu^2. \tag{15}$$

The stream function $\psi(x,y)$ satisfies the continuity equation (1) automatically with

$$u = \frac{\partial\psi}{\partial y} \quad v = -\frac{\partial\psi}{\partial x}. \tag{16}$$

Substitution of equations (10)–(14) into the governing momentum, angular momentum and energy equations leads to

$$(1+\Delta)F''' + \frac{3}{4}FF'' - \frac{1}{2}F'F' + \Delta G' + \theta = \xi\left(F'\frac{\partial F'}{\partial\xi} - F''\frac{\partial F}{\partial\xi}\right) \tag{17}$$

$$\lambda G'' + \frac{3}{4}FG' - \frac{1}{4}F'G - \Delta B\xi^{1/2}(2G+F'') = \xi\left(F'\frac{\partial G}{\partial\xi} - G'\frac{\partial F}{\partial\xi}\right) \tag{18}$$

$$\frac{1}{Pr}\theta'' + \frac{3}{4}F\theta' = \xi\left(F'\frac{\partial\theta}{\partial\xi} - \theta'\frac{\partial F}{\partial\xi}\right). \tag{19}$$

In the foregoing equations, the primes indicate partial differentiation with respect to η alone; $Pr = \nu/\alpha$ is the Prandtl number; and the dimensionless parameters Δ, B and λ, respectively, characterize the vortex viscosity, micro-inertia density and spin-gradient viscosity, defined as

$$\Delta = \frac{\kappa}{\mu}, \quad B = \frac{L^2}{jGr^{1/2}}, \quad \lambda = \frac{\gamma}{\mu j}. \tag{20}$$

Moreover, from the thermodynamic restrictions, the micropolar fluid parameters must satisfy the Clausius–Duhem inequalities given in Eringen [2] and adopted by Jena and Mathur [5] to satisfy the various materials. According to these inequalities, Δ, B, λ, Pr are all non-negative [5].

After the transformation, equations (5) and (9) become

$$F' = 0 \quad F + \frac{3}{4}\xi\frac{\partial F}{\partial\xi} = 0$$

$$G + \frac{1}{2}F''' = 0 \quad p\xi^{-1/4}\theta' = \theta - 1 \quad \text{at } \eta = 0 \tag{21a}$$

$$F' = 0 \quad G = 0 \quad \theta = 0 \quad \text{as } \eta \to \infty \tag{21b}$$

where $p = K_f bGr^{1/4}/K_s L$ is the conjugate heat transfer parameter. It should be noticed that for the limit case $p = 0$, the thermal boundary condition (21a) on the plate becomes isothermal. Hence, the magnitude of the parameter p determines the importance of the wall heat conduction effect. Moreover, for Newtonian fluid flow ($\Delta = 0$), equations (17) and (19) governing the micropolar fluid flow reduce to those of Pozzi and Lupo [17] in their study of the conjugate heat transfer characteristic of a Newtonian fluid flow along a vertical flat plate. In this case, equation (18) has no significance and can be omitted.

The physical quantities of primary interest in this problem include the skin friction coefficient C_f, the dimensionless wall couple stress M_w, the local Nusselt number Nu_x, the average Nusselt number $\overline{Nu}$ and the interfacial temperature distribution $\theta_w(=T_w-T_\infty/T_b-T_\infty)$. The first three quantities are defined, respectively, by

$$C_f = \frac{2\tau_w}{\rho U_c^2}, \quad M_w = \frac{m_w}{\rho U_c^2 L}, \quad Nu_x = \frac{q_w x}{K_f(T_b - T_\infty)} \tag{22}$$

where $U_c = \nu Gr^{1/2}\xi^{1/2}/L$ is the characteristic velocity.

With the aid of equations (10)–(14), along with the

definitions of the wall shear stress $\tau_w = [(\mu+\kappa)\partial u/\partial y + \kappa N]_{y=0}$ as well as the wall couple stress $m_w = \gamma(\partial N/\partial y)_{y=0}$, and the use of Fourier's law $q_w = -K_f(\partial T/\partial y)_{y=0}$, it follows that

$$C_f Gr_x^{1/4} = 2(1+0.5\Delta)F''(\xi,0) \tag{23}$$

$$M_w Gr_x^{1/2} = \frac{\lambda}{B}\xi^{1/2}G'(\xi,0) \tag{24}$$

$$Nu_x/Gr_x^{1/4} = -\theta'(\xi,0) \tag{25}$$

where $Gr_x = g\beta(T_b - T_\infty)x^3/\nu^2$. The average Nusselt number $\overline{Nu}$ is defined as $\overline{Nu} = \bar{h}L/K_f$, where $\bar{h}$ is the average heat transfer coefficient over the length L of the plate. In terms of non-dimensional variables, we have

$$\overline{Nu}/Gr^{1/4} = -\int_0^1 \xi^{-1/4}\theta'(\xi,0)\,d\xi. \tag{26}$$

NUMERICAL METHOD

To obtain a solution to the problem, the resulting system of nonlinear equations (17)–(19) and associated boundary conditions (21) must be solved simultaneously because of the coupling of the system. The solution of the system of steady equations was obtained by using a pseudotransient formulation approach in which a false transient term was introduced to each equation [20, 23]. We then solved these coupled nonlinear partial differential equations by using the cubic spline collocation method [20, 23–25] in conjunction with finite difference approximation. The main advantages of using a cubic spline collocation are shown in Refs [20, 25] and are, therefore, omitted here.

Equations (17)–(19) using the false transient technique in discretized form are

$$\frac{u_{i,j}^{n+1}-u_{i,j}^n}{\Delta\tau} = (1+\Delta)L_{u_{i,j}}^{n+1} + \left(\frac{3}{4}F_{i,j}^n + \xi_i\frac{F_{i,j}^n - F_{i-1,j}^n}{\Delta\xi_i}\right)l_{u_{i,j}}^{n+1} - \frac{1}{2}u_{i,j}^n u_{i,j}^n + \Delta l_{G_{i,j}}^n + \theta_{i,j}^{n+1} - \xi_i u_{i,j}^n\frac{u_{i,j}^n - u_{i-1,j}^n}{\Delta\xi_i} \tag{27}$$

$$\frac{G_{i,j}^{n+1}-G_{i,j}^n}{\Delta\tau} = \lambda L_{G_{i,j}}^{n+1} + \left(\frac{3}{4}F_{i,j}^{n+1} + \xi_i\frac{F_{i,j}^{n+1} - F_{i-1,j}^{n+1}}{\Delta\xi_i}\right)l_{G_{i,j}}^{n+1} - \frac{1}{4}u_{i,j}^{n+1}G_{i,j}^n - \Delta B\xi_i^{1/2}(2G_{i,j}^n + l_{u_{i,j}}^{n+1}) - \xi_i u_{i,j}^{n+1}\frac{G_{i,j}^n - G_{i-1,j}^n}{\Delta\xi_i} \tag{28}$$

$$\frac{\theta_{i,j}^{n+1}-\theta_{i,j}^n}{\Delta\tau} = \frac{1}{Pr}L_{\theta_{i,j}}^{n+1} + \left(\frac{3}{4}F_{i,j}^n + \xi_i\frac{F_{i,j}^n - F_{i-1,j}^n}{\Delta\xi_i}\right)l_{\theta_{i,j}}^{n+1} - \xi_i u_{i,j}^n\frac{\theta_{i,j}^n - \theta_{i-1,j}^n}{\Delta\xi_i} \tag{29}$$

where

$$l_u = \frac{\partial u}{\partial\eta} \quad L_u = \frac{\partial^2 u}{\partial\eta^2}$$

$$l_G = \frac{\partial G}{\partial\eta} \quad L_G = \frac{\partial^2 G}{\partial\eta^2}$$

$$l_\theta = \frac{\partial\theta}{\partial\eta} \quad L_\theta = \frac{\partial^2\theta}{\partial\eta^2}$$

$$\Delta\xi_i = \xi_i - \xi_{i-1}$$

$\Delta\tau = \tau^{n+1} - \tau^n$ represents the false time step, the subscript u stands for $\partial F/\partial\eta$ and the superscript n denotes the iteration order.

After some rearrangement, equations (27)–(29) can be expressed in the following spline approximation form:

$$\phi_{i,j}^{n+1} = Q_{i,j} + R_{i,j}l_{\phi_{i,j}}^{n+1} + S_{i,j}L_{\phi_{i,j}}^{n+1} \tag{30}$$

where ϕ represents the functions u, G and θ. The quantities $Q_{i,j}$, $R_{i,j}$ and $S_{i,j}$, are known coefficients, which are calculated at previous time steps (Table 1).

In this analysis, the cubic spline collocation method is used to generate an algorithm resulting in a single tridiagonal system containing either the function values at the grid points, the first derivatives, or the second derivatives only. Using cubic spline relations described by Rubin and Khosla [24], equation (30) at

Table 1. The coefficients of equation (30)

ϕ	Q	R	S
u	$\Delta\tau[-\frac{1}{2}u_{i,j}^n u_{i,j}^n + \Delta l_{G_{i,j}}^n + \theta_{i,j}^{n+1} - \xi_i u_{i,j}^n(u_{i,j}^n - u_{i-1,j}^n)/\Delta\xi_i] + u_{i,j}^n$	$\Delta\tau[\frac{3}{4}F_{i,j}^n + \xi_i(F_{i,j}^n - F_{i-1,j}^n)/\Delta\xi_i]$	$\Delta\tau(1+\Delta)$
G	$\Delta\tau[-\frac{1}{4}u_{i,j}^{n+1}G_{i,j}^n - \Delta B\xi_i^{1/2}(2G_{i,j}^n + l_{u_{i,j}}^{n+1}) - \xi_i u_{i,j}^{n+1}(G_{i,j}^n - G_{i-1,j}^n)/\Delta\xi_i] + G_{i,j}^n$	$\Delta\tau[\frac{3}{4}F_{i,j}^{n+1} + \xi_i(F_{i,j}^{n+1} - F_{i-1,j}^{n+1})/\Delta\xi_i]$	$\Delta\tau\lambda$
θ	$-\Delta\tau\xi_i u_{i,j}^n(\theta_{i,j}^n - \theta_{i-1,j}^n)/\Delta\xi_i + \theta_{i,j}^n$	$\Delta\tau[\frac{3}{4}F_{i,j}^n + \xi_i(F_{i,j}^n - F_{i-1,j}^n)/\Delta\xi_i]$	$\Delta\tau/Pr$

$(n+1)$th iteration may be written in the tridiagonal form as

$$a_{i,j}\phi_{i,j-1}^{n+1}+b_{i,j}\phi_{i,j}^{n+1}+c_{i,j}\phi_{i,j+1}^{n+1}=d_{i,j} \tag{31}$$

where ϕ represents the function (u, G, θ) and its first- and second-order derivatives. Therefore, equation (31) can be easily solved by the Thomas algorithm.

The computational procedure followed is first to solve the energy equation, which provides the temperature field necessary for the solution of the reduced stream function equation. Solution of the transformed angular momentum equation for G then completes the procedure. This cycle of computation is repeated until convergence is achieved. The criterion for the convergence of the solutions is that the maximum relative change in all the dependent variables satisfy

$$\frac{|\phi_{i,j}^{n+1}-\phi_{i,j}^{n}|_{\max}}{|\phi_{i,j}^{n}|_{\max}}<5\times10^{-7} \tag{32}$$

RESULTS AND DISCUSSION

Equations (17)–(19) reveal that the governing nondimensional parameters of the problem are Δ, B, λ, Gr, Pr and p. In order to reduce the number of parameters involved, a parametric study was carried out for the cases of $B=5\times10^4$, $\lambda=5.0$ and $Gr=1.2\times10^5$ with the vortex viscosity parameter Δ ranging from 0.0 to 5.0, the Prandtl number parameter Pr from 0.7 to 20.0, and the conjugate heat transfer parameter p from 0 to 0.3. These values satisfy the thermodynamic restrictions on the material parameters given by Eringen [2].

Since no experimental data to the problem of conjugate free convection flow of micropolar fluids has been reported in the literature, computations were first carried out for the conjugate free convection flow of Newtonian fluids along a vertical flat plate, corresponding to the case computed by Pozzi and Lupo [17] for $\Delta=0$ and $Pr=2.97$ to assess the accuracy of the present numerical solution. Table 2 shows that the solid–liquid interfacial temperature $\theta(\xi,0)$ (as a function of ξ) obtained in the present study are identical to those obtained by Pozzi and Lupo [17].

Representative dimensionless interfacial temperature distributions as a function of the streamwise coordinate ξ are plotted in Fig. 2 for four different values of p with $Pr=6.0$ and $\Delta=1.0$. It is also remarked that the present analysis includes the case of laminar free convection flow of micropolar fluids along an isothermal vertical flat plate. This corresponds to the case of $p=0$. Equation (21a) for θ under this circumstance reduces to $\theta(\xi,0)=1$. It is seen from the figure that for a given p, the temperature of the fluid on the surface increases monotonically with increasing ξ. This figure also reveals that higher values of p lead to larger surface temperature variations. The primary cause of this behavior is that larger values of p correspond to lower wall conductance K_sL and higher convective cooling (great K_f and Gr), which promote greater surface temperature variations.

Table 2. A comparison of the $\theta(\xi,0)$ for $Pr=2.97$, $p=0.4$ and $\Delta=B=\lambda=0$ (Newtonian fluid)

	$\theta(\xi,0)$	
ξ	Pozzi and Lupo [17]	Present results
0.002	0.490	0.490
0.016	0.620	0.621
0.032	0.658	0.659
0.064	0.693	0.696
0.096	0.714	0.716
0.159	0.739	0.740
0.237	0.762	0.760

Figure 3 depicts the variation of the dimensionless interfacial temperature profiles with ξ for selected values of Δ. Notice that the solutions plotted in Fig. 3 for the limiting case of $\Delta=0$, which corresponds to the case of Newtonian fluids. It is found that the dimensionless interfacial temperature is higher for the micropolar fluids as compared with the Newtonian fluids. The higher the value of Δ, the higher is the dimensionless interfacial temperature for fixed values of Pr and p. Also, the dimensionless interfacial temperature increases as ξ increases.

Figure 4 shows the streamwise variation of the interfacial temperature profiles for various values of the Prandtl number Pr. The results indicate an increase of Pr gives rise to greater surface temperature variations. The reason for this behavior is that the larger the Pr, the higher is the heat transfer coefficients.

The variation of the wall shear stress τ_w expressed in terms of local skin friction factor along the streamwise coordinate is shown in Fig. 5 for different values of p. The dashed horizontal line ($p=0$) is for the isothermal plate, while the solid lines for $p>0$ are for nonisothermal plates, with larger temperature variations being evoked by larger p. Thus, the more nonisothermal the plate, the lower is the local skin friction factor. In all cases, the skin friction factor increases in the direction of fluid flow. The above behavior is a consequence of the fact that in the case of free convection, the streamwise increase of the temperature of the plate which causes in the buoyancy (driving force), leading to an additional acceleration of the flow.

To investigate the influence of the micropolar material parameter Δ on the skin friction factor, numerical results are plotted in Fig. 6 for $Pr=6.0$. An inspection of the figure reveals that the local skin friction factor is almost independent of ξ and varies strongly with the micropolar material parameter Δ. It is also observed that as Δ increases for fixed values of Pr and p, the skin friction factor decreases. In addition, the results show that the skin friction factor is higher in the case of Newtonian fluids ($\Delta=0$) than that of micropolar fluids. This is because the micropolar fluids offer greater resistance (resulting from

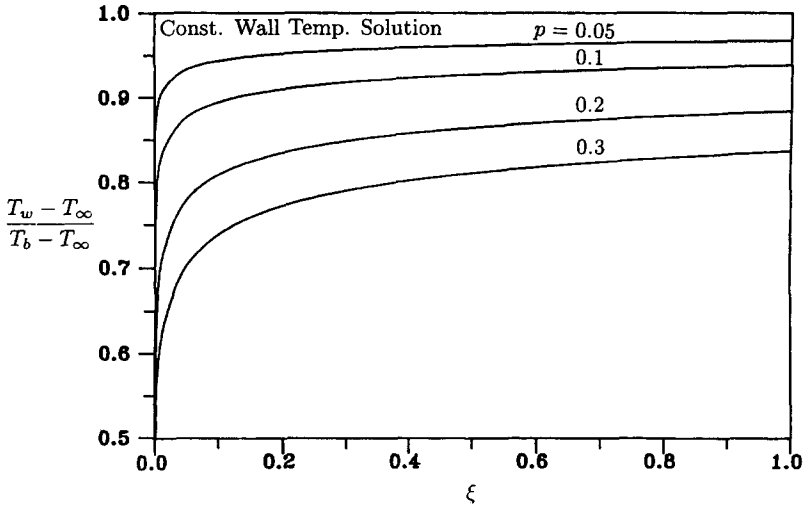

Fig. 2. Variation of interfacial temperature profiles with ξ at different values of p for $Pr = 6.0$ and $\Delta = 1.0$.

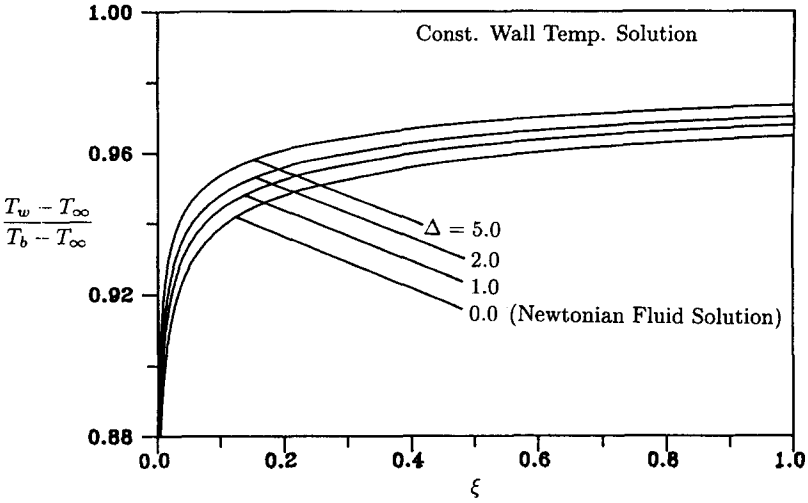

Fig. 3. Variation of interfacial temperature profiles with ξ at different values of Δ for $Pr = 6.0$ and $p = 0.05$.

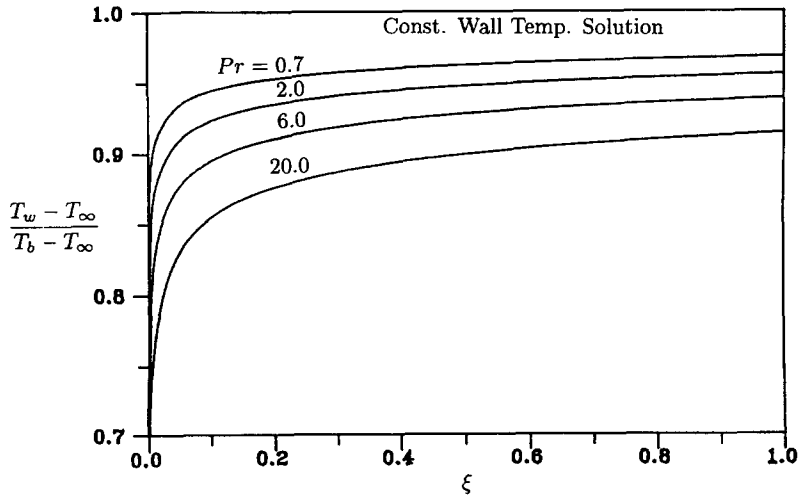

Fig. 4. Variation of interfacial temperature profiles with ξ at different values of Pr for $\Delta = 1.0$ and $p = 0.1$.

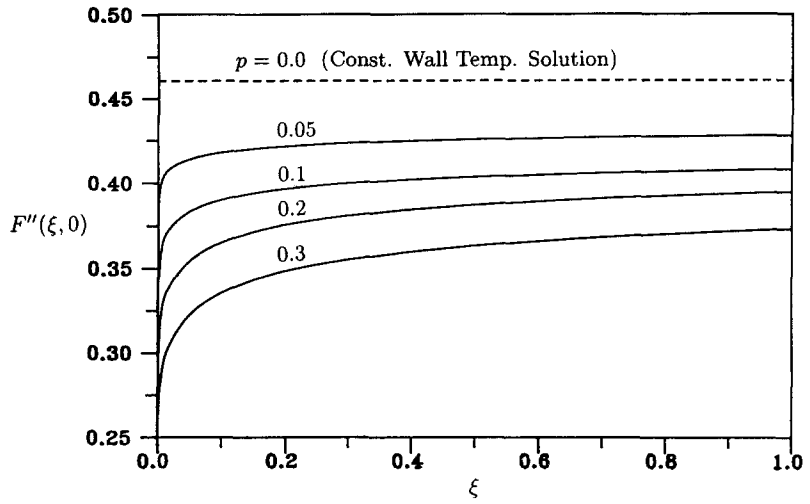

Fig. 5. Effect of p on the skin friction parameter for $Pr = 6.0$ and $\Delta = 1.0$.

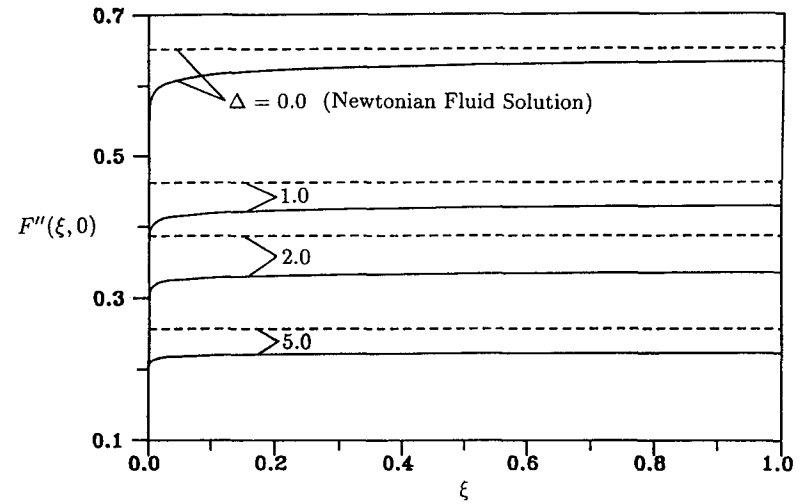

Fig. 6. Effect of Δ on the skin friction parameter for $Pr = 6.0$; dashed lines, $p = 0.0$; solid lines, $p = 0.05$.

dynamic viscosity and vortex viscosity) to the fluid motion when compared to a Newtonian fluid.

In Fig. 7 the effect of Pr on the skin friction factor is shown for $\Delta = 1.0$. The dashed lines in the figure indicate the skin friction factor corresponding to the cases of isothermal flat plate. From the figure, it can be seen that the local friction factor decreases with increasing value of Pr. A increase in the Prandtl number implies a higher density of fluid which exhibits a smaller sensitivity to the buoyancy force effect, thereby causing a smaller change in the velocity gradients at the flat plate. The influence of conjugate heat transfer parameter p on the skin friction factor is more pronounced for smaller Prandtl numbers.

To show the effect of the conjugate heat transfer parameter p on the wall couple stress expressed by $G'(\xi,0)$, the curves are shown in Fig. 8 for $Pr = 6.0$ and $\Delta = 1.0$. The result reveals that the wall couple stress increases with ξ, but decreases as p increases. This is due to greater surface temperature differences with the ambient as ξ increases or p decreases which results in higher the wall couple stress. The influences of the micropolar material parameter Δ and the Prandtl number Pr on the streamwise variations of the wall couple stress are plotted in Figs 9 and 10, respectively. It is revealed from these two figures that increase in the value of Δ or Pr reduces the wall couple stress.

Representative distributions of the heat flow rate expressed by $Nu_x/Gr_x^{1/4}$ along the streamwise direction are presented in Fig. 11 for various values of p at $Pr = 6.0$ and $\Delta = 1.0$. The dashed line in the figure indicates the local heat transfer rate corresponding to the case of isothermal flat plate. The local heat transfer rate increases with increasing ξ. Also, from Fig. 11 it may be noted that the influence of the conjugate heat transfer parameter p is to decrease the local heat transfer rate. This decrease increases with increasing p. This is in agreement with the interfacial temperature distributions given in Fig. 2.

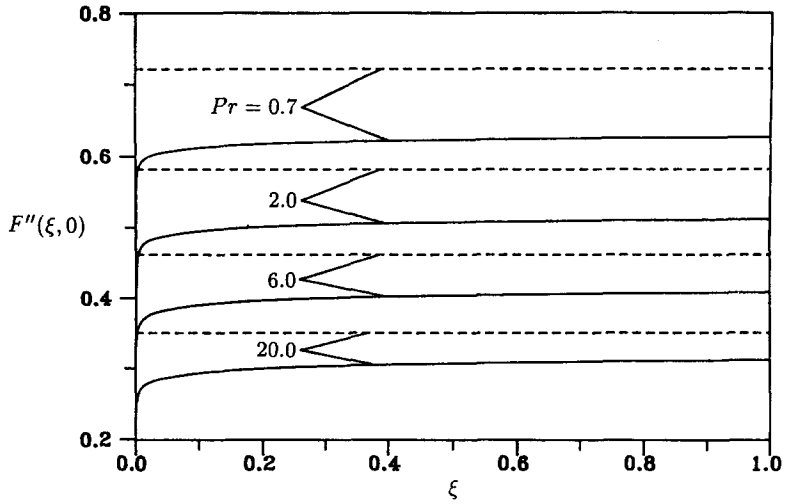

Fig. 7. Effect of Prandtl number on the skin friction parameter for $\Delta = 1.0$; dashed lines, $p = 0.0$; solid lines, $p = 0.1$.

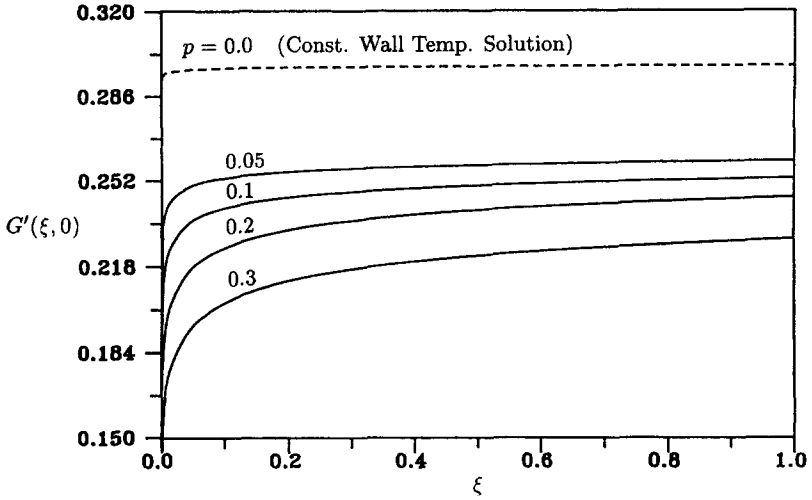

Fig. 8. Effect of p on the wall couple stress parameter for $Pr = 6.0$ and $\Delta = 1.0$.

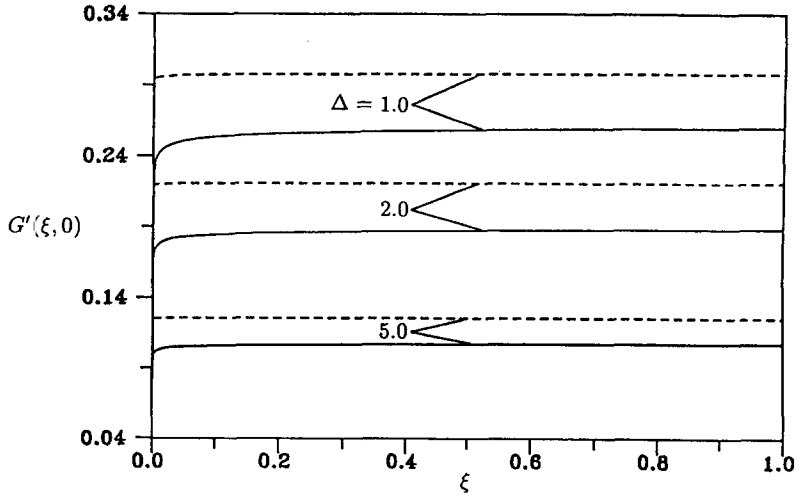

Fig. 9. Effect of Δ on the wall couple stress parameter for $Pr = 6.0$; dashed lines, $p = 0.0$; solid lines, $p = 0.05$.

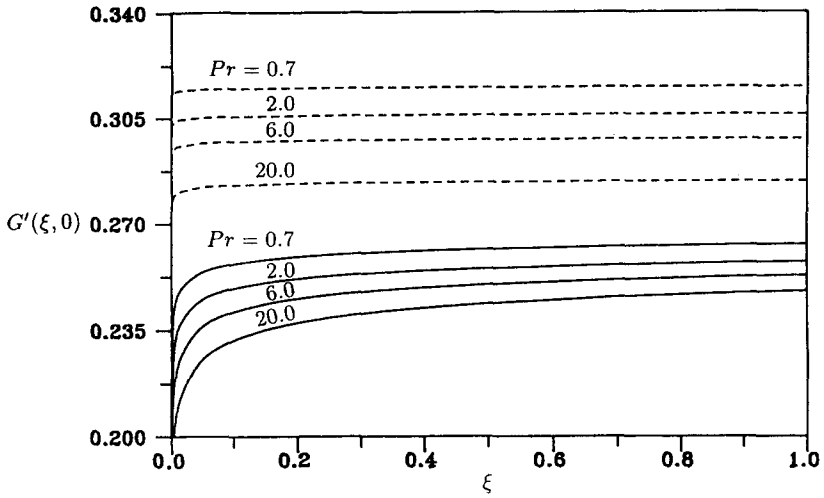

Fig. 10. Effect of Prandtl number on the wall couple stress parameter for $\Delta = 1.0$; dashed lines, $p = 0.0$; solid lines, $p = 0.1$.

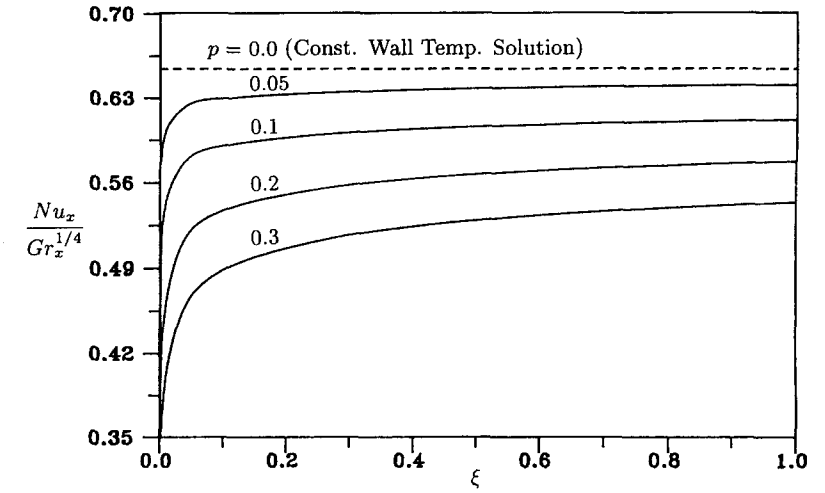

Fig. 11. Effect of p on the heat transfer rate for $Pr = 6.0$ and $\Delta = 1.0$.

Figure 12 gives the plot of the local heat transfer rate for different values of the micropolar material parameter Δ. The curves illustrated that as the value of Δ increases, the local heat transfer rate decreases. This is because that as Δ increases, the thermal boundary layer becomes larger and, thus, gives rise to a smaller value of the local heat transfer rate. The effect of wall conduction is more pronounced for smaller micropolar material parameters.

Figure 13 shows the distributions of the local heat transfer rate for different values of the Prandtl number Pr. The dashed lines ($p = 0$) in the figure indicate the corresponding curves for the case of isothermal plate. From Fig. 13, the results show that the higher the value of the Prandtl number Pr, the larger is the departure of the local heat transfer rate from the constant wall temperature solution. The effect of wall conduction on the heat transfer rate is more pronounced when Pr is large. In addition, Fig. 13 also reveals that for a given value of Δ, micropolar fluids with larger Prandtl numbers yield higher local heat transfer rate. This is because a larger Prandtl number gives rise to a larger wall temperature gradient and, hence, a larger heat transfer rate.

The average Nusselt number results $\overline{Nu}/Gr^{1/4}$ are tabulated in Table 3 for different values of p and Δ at $Pr = 6.0$. The numerical values indicate that increasing the value of p or Δ results in a decrease in the values of $\overline{Nu}/Gr^{1/4}$. Table 4 displays the effect of the Prandtl number Pr on the average Nusselt number results $\overline{Nu}/Gr^{1/4}$. As the Prandtl number increases, the average Nusselt number results increase. From Tables 3 and 4, we conclude that under the influences of p, Δ and Pr, the behavior of the average Nusselt number is similar to that of the local Nusselt number.

CONCLUSIONS

In this study, the effect of wall conduction on laminar natural convection flow of micropolar fluids along

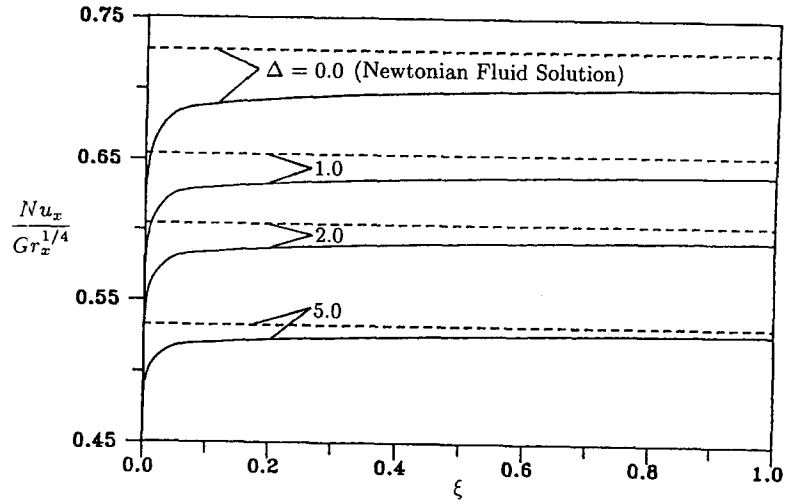

Fig. 12. Effect of Δ on the heat transfer rate for $Pr = 6.0$; dashed lines, $p = 0.0$; solid lines, $p = 0.05$.

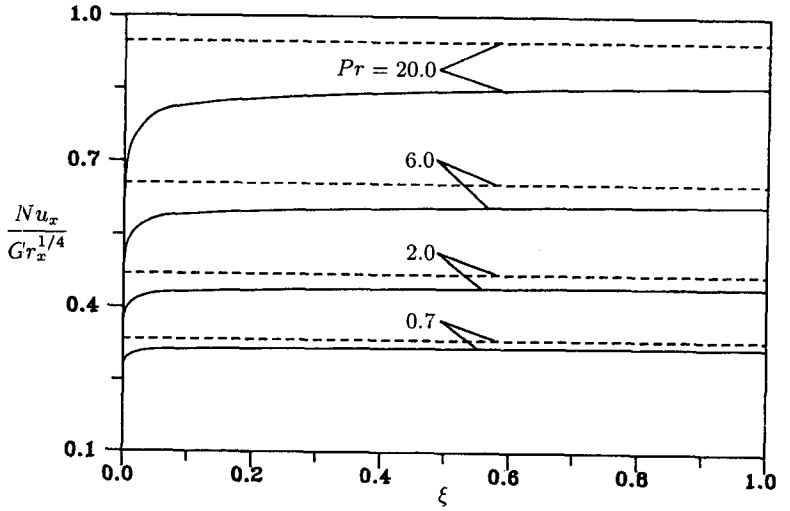

Fig. 13. Effect of Prandtl number on the heat transfer rate for Δ = 1.0; dashed lines, $p = 0.0$; solid lines, $p = 0.1$.

Table 3. Effect of p and Δ on the average Nusselt number results $\overline{Nu}/Gr^{1/4}$ for $Pr = 6.0$

	Δ = 1.0		p = 0.05
p	$\overline{Nu}/Gr^{1/4}$	Δ	$\overline{Nu}/Gr^{1/4}$
0.0	0.87825	0.0	0.93012
0.05	0.84977	0.5	0.87760
0.1	0.80117	1.0	0.84977
0.2	0.73941	2.0	0.78801
0.3	0.68282	5.0	0.70144

Table 4. Effect of Pr on the average Nusselt number results $\overline{Nu}/Gr^{1/4}$ for Δ = 1.0

	$\overline{Nu}/Gr^{1/4}$	
Pr	$p = 0.0$	$p = 0.1$
20.0	1.27226	1.11226
6.0	0.87825	0.80117
2.0	0.62809	0.58340
0.7	0.44600	0.42147

a vertical flat plate is analyzed. Numerical results to the transformed boundary layer equations have been obtained by using the cubic spline collocation method. Of interest are the influences of the conjugate heat transfer parameter, the micropolar material parameter, and the Prandtl number on the solid–liquid interfacial temperature distribution, the local skin friction factor, the wall couple stress and the local heat transfer rate. The following results have been obtained:

(1) The conjugate heat transfer parameter has a substantial effect on the micropolar fluid flow field and, thus, on the heat transfer rate as compared to the isothermal plate case (without the effect of wall conduction). An increase in the conjugate heat transfer parameter results in a decrease in the interfacial

temperature distribution, the skin friction factor, the wall couple stress and the local heat transfer rate. Moreover, the interfacial temperature increases monotonically along the streamwise direction.

(2) In comparison to a Newtonian fluid, the micropolar fluid is found to have smaller the skin friction factor and the local heat transfer rate and a higher interfacial temperature, especially for higher micropolar effect.

(3) As the Prandtl number increases, the interfacial temperature variation and heat transfer rate increase, while the skin friction factor and wall couple stress decrease.

(4) The effect of wall conduction on the local heat transfer rate is more pronounced when the Prandtl number is large or micropolar material parameter is small.

Acknowledgement—The authors are grateful to the referees for their valuable comments and, thus, the improvement of this paper.

REFERENCES

1. Eringen, A. C., Simple microfluids. *International Journal of Engineering Science*, 1964, **2,** 205–217.
2. Eringen, A. C., Theory of thermomicrofluids. *Journal of Mathematic Analysis Applications*, 1972, **38,** 480–496.
3. Ariman, T., Turk, M. A. and Sylvester, N. D., Microcontinuum fluid mechanics—a review. *International Journal of Engineering Science*, 1973, **11,** 905–930.
4. Ahmadi, G., Self-similar solution of imcompressible micropolar boundary layer flow over a semi-infinite plate. *International Journal of Engineering Science*, 1976, **14,** 639–646.
5. Jena, S. K. and Mathur, M. N., Similarity solutions for laminar free convection flow of a thermomicropolar fluid past a non-isothermal vertical flat plate. *International Journal of Engineering Science*, 1981, **19,** 1431–1439.
6. Soundalgekar, V. M. and Takhar, H. S., Flow of micropolar fluid past a continuously moving plate. *International Journal of Engineering Science*, 1983, **21,** 961–965.
7. Gorla, R. S. R. and Ameri, A., Boundary layer flow of a micropolar fluid on a continuous moving cylinder. *Acta Mechanica*, 1985, **57,** 203–214.
8. Gorla, R. S. R., Combined forced and free convection in micropolar boundary layer flow on a vertical flat plate. *International Journal of Engineering Science*, 1988, **26,** 385–391.
9. Gorla, R. S. R., Lin, P. P. and Yang, A. J., Asymptotic boundary layer solutions for mixed convection from a vertical surface in a micropolar fluid. *International Journal of Engineering Science*, 1990, **28,** 525–533.
10. Hassanien, I. A. and Gorla, R. S. R., Heat transfer to a micropolar fluid from a non-isothermal stretching sheet with suction and blowing. *Acta Mechanica*, 1990, **84,** 191–199.
11. Kelleher, M. D. and Yang, K. T., A steady conjugate heat transfer problem with conduction and free convection. *Applied Science Research*, 1967, **17,** 249–269.
12. Lock, G. S. H. and Gunn, J. C., Laminar free convection from a downward-projecting fin. *Journal of Heat Transfer*, 1968, **90,** 63–70.
13. Ziness, A. E., The coupling of conduction with laminar convection from a vertical plate with arbitrary surface heating. *Journal of Heat Transfer*, 1970, **92,** 528–535.
14. Chida, K. and Katto, Y., Study on conjugate heat transfer by vectorial dimensional analysis. *International Journal of Heat and Mass Transfer*, 1976, **19,** 453–460.
15. Miyamoto, M., Sumikawa, J., Akiyoshi, T. and Nakamura, T., Effects of axial heat conduction in a vertical flat plate on free convection heat transfer. *International Journal of Heat and Mass Transfer*, 1980, **23,** 1545–1553.
16. Timma, J. and Padet, J. P., Etude theorique du couplage convection–conduction en convection libre laminaire sur une plaque plane verticale. *International Journal of Heat and Mass Transfer*, 1985, **28,** 1097–1104.
17. Pozzi, A. and Lupo, M., The coupling of conduction with laminar natural convection along a flat plate. *International Journal of Heat and Mass Transfer*, 1988, **31,** 1807–1814.
18. Kim, S. H., Anand, N. K. and Aung, W., Effect of wall convection on free convection between asymmetrically heated vertical plates: uniform wall heat flux. *International Journal of Heat and Mass Transfer*, 1990, **33,** 1013–1023.
19. Anand, N. K., Kim, S. H. and Aung, W., Effect of wall convection on free convection between asymmetrically heated vertical plates: uniform wall temperature. *International Journal of Heat and Mass Transfer*, 1990, **33,** 1025–1028.
20. Char, M. I., Chen, C. K. and Cleaver, J. W., Conjugate forced convection heat transfer from a continuous, moving flat sheet. *International Journal of Heat and Fluid Flow*, 1990, **11,** 257–261.
21. Vynnycky, M. and Kimura, S., Conjugate free convection due to a heated vertical plate. *International Journal of Heat and Mass Transfer*, 1996, **39,** 1067–1080.
22. Na, T. Y., Effect of wall conduction on natural convection over a vertical slender hollow circular cylinder. *Applied Science Research*, 1995, **54,** 39–50.
23. Rubin, S. G. and Graves, R. A., Viscous flow solution with a cubic spline approximation. *Computers and Fluids*, 1975, **3,** 1–36.
24. Rubin, G. S. and Khosla, P. K., Higher-order numerical solutions using cubic splines. *AIAA*, 1976, **14,** 851–858.
25. Wang, P. and Kahawita, R., Numerical integration of partial differential equations using cubic splines. *International Journal of Computer Mathematics*, 1983, **13,** 271–286.